Decentralized Navigation for Heterogeneous Swarm Robots With Limited Field of View

Ryuma Maeda, Takahiro Endo, and Fumitoshi Matsuno

***Abstract*—This letter proposes a navigation method for multi-robots with heterogeneous abilities. In this method, a single leader navigates other robots that have different translational and rotational velocity and acceleration, sensing distance and angle while maintaining global connectivity. In particular, this method is decentralized in which the leader does not need real-time information on the whole swarm, and all followers use only locally available information to follow a target. Validity and effectiveness of the proposed method are demonstrated by theoretical analysis, and in a simulation and an experiment with real robots.**

***Index Terms*—Distributed robot systems, swarms, wheeled robots.**

I. Introduction

In RECENT years, swarm robotics have been attracting a great deal of attention. A robotic swarm has advantages such as robustness against individual losses, flexibility for environments or tasks, and scalability, allowing for increase of robot number [1]–[4]. In particular, scalability can be achieved with a decentralized method, in which the agents act according to locally available information, in contrast to a centralized method in which the information of the whole swarm is managed by a central computer. In a decentralized method, each agent of a robotic swarm basically follows a simple control law, which can result in high-quality performance of the whole swarm based on interactions between agents. Due to these characteristics, it is expected that swarm robots will be applicable to various situations.

There are many environments and tasks that could benefit from the advantages of swarm robots including cooperative coverage [5], surveillance [6], target-capturing [7], and transportation [8]. For these practical applications, swarm robots need to move as a flock to a desired location. To control multi-robots in a flock in a decentralized way, it is necessary for each robot to obtain information about neighboring agents using onboard sensors or wireless communication equipment. However, there is an upper limit to the distance at which a robot can acquire information from other agents. Therefore, each robot must remain within the sensing region of the neighboring agents in order to maintain the flock.

Although many studies have investigated connectivity maintenance of swarm robots [9]–[11], most of them have focused on a homogeneous swarm in which all robots have the same performance. However, multi-agent systems composed of robots with different abilities or functions have the potential to handle a wider variety of tasks by cooperating with each other while making use of each individual's characteristics [12], [13]. For instance, a previous study [14] considered connectivity maintenance of a heterogeneous swarm consisting of robots with different sensing ranges and mobility, and proposed a decentralized method for navigating the swarm while maintaining connectivity. However, it assumed that all agents could sense every direction.

Most sensors and cameras are limited not only by distance, but also by angle in the sensing region. Because of these constraints, if we apply the method for robots with omni-directional sensing ability to those that cannot sense every direction, we cannot ensure that connectivity of the whole swarm is maintained. Some studies have also proposed control strategies to navigate robots using cameras with angle constraints [15], [16]. Although they ensure maintenance of connectivity and collision avoidance between agents, the swarm is composed of homogeneous robots. On the other hand, [17] proposed a decentralized algorithm to obtain a minimum connected graph of a whole swarm, consisting of heterogeneous robots equipped with cameras with different sensing distances and angles. The main focus of this research, however, was to achieve the minimum strongly connected graph. Therefore, it did not take the physical movement of robots into consideration, and thus it could not deal with heterogeneous abilities such as maximum velocity and acceleration.

In this letter, we propose a decentralized connectivity-maintenance method for a heterogeneous swarm. Each robot in the swarm has its own unique maximum distance and angle of sensing range. In addition, we assume that each also has physical limitations in terms of maximum translational and rotational velocity and acceleration. With these characteristics, we consider the robots to be heterogeneous. In our strategy, a single leader navigates the other followers. Although the leader has knowledge regarding the specifications of all agents, it has no access to real-time information for the whole swarm. The leader has no constraint but maximum translational speed, which means it can move freely under the speed restriction. On the other hand, each follower selects a target robot, and follows it while preserving its physical limitations. Each follower moves depending only on local information, such as relative position from its target and its own specifications. Thus, we treat the problem as a two-body problem with unidirectional interaction.

Manuscript received September 10, 2016; revised December 3, 2016; accepted January 1, 2017. Date of publication January 17, 2017; date of current version February 9, 2017. This letter was recommended for publication by Associate Editor S. Carpin and Editor N. Y. Chong upon evaluation of the reviewers' comments. This work was supported in part by JSPS KAKENHI under Grant Number 26249024.

The authors are with the Department of Mechanical Engineering and Science, Kyoto University, Kyoto daigaku-katsura, Nishikyo-ku, Kyoto 615-8540, Japan (e-mail: ray501.itsme182@gmail.com; endo@me.kyoto-u.ac.jp; matsuno@me.kyoto-u.ac.jp).

Color versions of one or more of the figures in this letter are available online at http://ieeexplore.ieee.org.

Digital Object Identifier 10.1109/LRA.2017.2654549

The main contributions of this letter are as follows. First, we deal with a heterogeneous swarm, in which each robot has a different sensing range, limited field of view, performance, and physical limitations, such as maximum velocity and acceleration. Such robotic swarms have the potential to deal with a wider variety of tasks. Second, we propose a decentralized controller that allows the swarm to maintain connectivity during navigation. The proposed method is fully decentralized, which provides scalability. Third, the sensors mounted on the robots are not necessarily omnidirectional. In addition, the robots do not require communication equipment. To the best of our knowledge, this is the first work that offers all of these advantages. With our proposed method, robots with different mobile and sensing capabilities can flock. A good example of a real application of this method would be navigating different types of robots coming from different organizations by one leader robot.

This letter is organized as follows. In Section II, we present the problem, and the proposed method is introduced in Section III. Section IV describes the mathematical analysis used to prove the validity of the method. Sections V and VI provides the results from simulation and experiments with real robots, respectively, to confirm the feasibility of the method. Finally, Section VII concludes the letter.

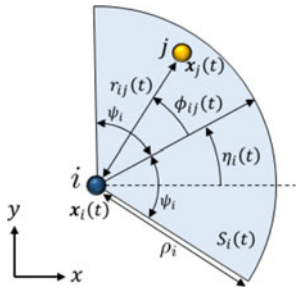

Fig. 1. Relative positions of agents j and i.

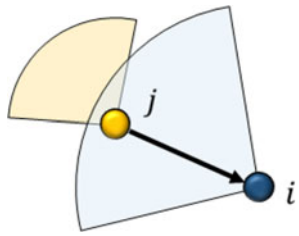

Fig. 2. ji semi-connection.

II. Problem Statement

The goal of this letter is to control a heterogeneous swarm of robots using a decentralized method that maintains connectivity under physical limitations. We assume the leader has knowledge regarding the specifications of all followers. However, the leader cannot access global real-time information, and the followers can obtain only local information from their own sensing.

A. Modeling

We consider $n+1$ agents in a two-dimensional plane $D \in \mathbb{R}^2$. ID $1, 2, \ldots, n$ are assigned to followers, and $n+1$ to the leader. Agents do not need to distinguish the IDs of others. Let $\mathcal{A} := \{1, 2, ..., n+1\}$, and $\mathcal{F} := \{1, 2, ..., n\}$. The position vector and orientation of agent $i \in \mathcal{A}$ at time t are $\boldsymbol{x}_i(t) = [x_i(t),\ y_i(t)]^\top$ and $\eta_i(t)$, respectively, and the dynamics of agent i are described as

$$\dot{\boldsymbol{x}}_i(t) = \boldsymbol{u}_i(t), \tag{1}$$

$$\dot{\eta}_i(t) = \omega_i(t), \tag{2}$$

where $\boldsymbol{u}_i(t)$ is translational velocity input and $\omega_i(t)$ is rotational speed input. Follower $i \in \mathcal{F}$ has physical limitations as follows:

$$\|\boldsymbol{u}_i(t)\| \leq U_i, \tag{3}$$

$$\|\dot{\boldsymbol{u}}_i(t)\| \leq A_i, \tag{4}$$

$$|\omega_i(t)| \leq \Omega_i, \tag{5}$$

$$|\dot{\omega}_i(t)| \leq B_i, \tag{6}$$

$$\boldsymbol{u}_i(t), \omega_i(t) \text{ are continuous for any } t, \tag{7}$$

where U_i and A_i are the maximum speed and acceleration for translational movement, and Ω_i and B_i are those for rotation, respectively. Here, $\dot{\boldsymbol{u}}_i(t)$ is defined as the semi-derivative of $\boldsymbol{u}_i(t)$ with respect to t, whose norm is larger if $\boldsymbol{u}_i(t)$ is left or right semi-differentiable. $\dot{\omega}_i(t)$ is defined in the same way. The leader has no physical limitation except for the maximum translational speed described in Section III. We define the distance between position $\boldsymbol{x}(t) = [x(t),\ y(t)]^\top \in D$ and follower $i \in \mathcal{F}$ as $r_i(t) = \|\boldsymbol{x}(t) - \boldsymbol{x}_i(t)\|$. In addition, we define the bearing angle from follower i's orientation to $\boldsymbol{x}$ as $\phi_i(t) = \operatorname{atan2}\left(y(t) - y_i(t), x(t) - x_i(t)\right) - \eta_i(t)$. If agent $j \in \mathcal{A}$ is in the region

$$S_i(t) = \{\boldsymbol{x}(t) \in D \mid r_i(t) \leq \rho_i,\ |\phi_i(t)| \leq \psi_i\}, \tag{8}$$

follower i can measure the relative distance $r_{ij}(t) = \|\boldsymbol{x}_j(t) - \boldsymbol{x}_i(t)\|$ and orientation $\phi_{ij}(t) = \operatorname{atan2}(y_j(t) - y_i(t), x_j(t) - x_i(t)) - \eta_i(t)$. Here, ρ_i is the maximum sensing distance, and $2\psi_i$ is the angle of the sensing region of follower i (see Fig. 1).

B. Connectivity

We describe the relationship between the agents by graph representation. Let $\mathcal{N} := \{N_1, N_2, \ldots, N_{n+1}\}$ and $\mathcal{E}(t)$ be a set of nodes and a set of directed edges of digraph $\mathcal{G}(t)$, respectively. $E_{ij} \in \mathcal{E}(t)$ is an edge from N_i to N_j. We call N_i a *parent* of N_j if E_{ij} exists. A series of nodes $(N_{i_1}, N_{i_2}, \ldots, N_{i_l})$ is a directed path if $l \geq 2$ and $E_{i_k i_{k+1}}$ $(k = 1, 2, \ldots, l-1)$ exist. $\mathcal{G}(t)$ is a *spanning tree* whose *root* is N_{n+1} if every node in $\mathcal{N}$, except N_{n+1}, has exactly one parent, and directed paths from N_{n+1} to the other nodes exist. We apply this representation to the relationship between agents. A directed edge E_{ji} exists if and only if $\boldsymbol{x}_j(t) \in S_i(t)$, which describes the information flow.

Definition 1 (Leader Semi-Connected (LSC)): Agent i and j are ji semi-connected, or agent i is semi-connected with j, if E_{ji} exists (see Fig. 2). Agent i is *leader semi-connected (LSC)* if there is at least one directed path from N_{n+1} to N_i. Then it can also be said of the LSC swarm that $\mathcal{G}(t)$ includes a spanning tree whose root is N_{n+1}.

If a follower is always LSC, the effect of the leader's movement will propagate to the follower. Thus, the leader directs the follower.

Next, we assume initial conditions as follows.

Assumption 1 (Initial State): Let ρ_i', ρ_i'', and ρ_i''' be positive constants satisfying $0 < \rho_i''' < \rho_i'' < \rho_i' < \rho_i$. Concerning follower $i \in \mathcal{F}$, let us define the hatched region $S_i'(t)$

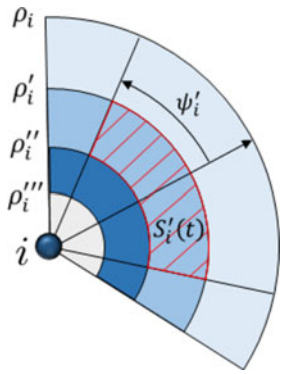

Fig. 3. Sensing region.

in Fig. 3 as

$$S_i'(t) = \{\boldsymbol{x}(t) \in D \mid \rho_i'' \le r_i(t) \le \rho_i',\ |\phi_i(t)| \le \psi_i'\}, \quad (9)$$

and $\partial S_i'(t)$ as the boundary of $S_i'(t)$. At the initial time $t = 0$, the swarm is LSC even if the sensing region of follower i is assumed to be $S_i'(0) \backslash \partial S_i'(0)$. In addition, all followers are stationary.

Assumption 1 is introduced to ensure that, after the leader starts moving, the swarm constructs a spanning tree without fail. Here, ψ_i' is defined as

$$\psi_i' = \psi_i - \frac{K_i^2}{2B_i}, \quad (10)$$

where ψ_i' is the upper limit of $|\phi_{ij}|$ at the initial state so that follower i can maintain connectivity right after it determines its target. $\rho_i'' < r_{ij} < \rho_i'$ is the distance at which at least one LSC agent is located at the initial time. This means that the larger the distance between ρ_i' and ρ_i'', the less restrictive the initial condition. ρ_i''' is the minimum distance between agent i and j, as explained in Section III and IV. The definition of K_i is described in Section III.

III. Proposed Method

In this section, we propose a method for constructing a spanning tree whose root is the leader, as well as for maintaining the tree. In our strategy, each follower selects another agent as its target, and stays semi-connected with that target. As a result, LSC of all followers in the swarm is achieved. Our method contains constraints on the leader's translational speed, determination of a target to follow, and design of the control law.

A. Constraints on the Leader

In order for the swarm to maintain LSC, the leader is required to move under the following speed restrictions:

$$U_{n+1} \le \min_{i \in \mathcal{F}} U_i, \quad (11)$$

$$U_{n+1} \le \min_{i \in \mathcal{F}} \frac{(\rho_i - \rho_i')A_i}{(2+\sqrt{2})U_i}, \quad (12)$$

$$U_{n+1} \le \min_{i \in \mathcal{F}} \rho_i''' K_{i\max}, \quad (13)$$

$$U_{n+1} \le \min_{i \in \mathcal{F}'} \frac{2a_i \rho_i' K_{i\max}}{3a_i - K_{i\max}}, \quad (14)$$

where we define $a_i = U_i/(\rho_i - \rho_i')$, $K_{i\max} = \min\{\Omega_i, \sqrt{\psi_i B_i/2}\}$, and $\mathcal{F}' = \{i \in \mathcal{F} \mid 3a_i > K_{i\max}\}$. Moreover, if any of the right sides of (11)–(14) concerning follower i is less than $\sqrt{(\rho_i'' - \rho_i''')A_i/2}$, we define V_i as the minimum value among them. If not, $V_i = \sqrt{(\rho_i'' - \rho_i''')A_i/2}$. We add the following restriction:

$$U_{n+1} \le \min_{i \in \mathcal{F}} \frac{(\rho_i'' - \rho_i''')A_i}{2V_i}. \quad (15)$$

As a result, V_i is equal to the minimum value of the right sides of (11)–(15) concerning follower i, and thus, $U_{n+1} \le V_i \le U_i$ holds for any i. V_i is introduced to make the right side of (15) lager, which eases the restriction (15). We also assume that the following conditions are satisfied:

$$0 < \rho_i'' < \rho_i' < \rho_i,\ \ \rho_i''' \in [(\sqrt{2}-1)\rho_i'', \rho_i''). \quad (16)$$

This condition is used to prove the maintenance of physical restriction in Section IV.

Physical constraint (11) is included to satisfy translational velocity constraint (3) for any followers, while constraints (12) and (15) are to satisfy (4). Conditions (13) and (14) are constraints to ensure that the gain k_i of control input (25), which demonstrates that condition (26) exists.

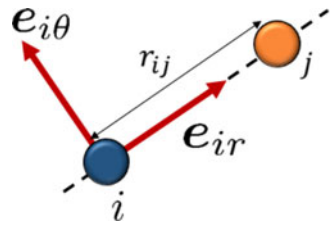

Fig. 4. Local basis vectors.

B. Target Determination

Follower $i \in \mathcal{F}$ determines its target as described below. At time $t > 0$, agent j that is first on $\partial S_i'(t)$ from $S_i(t) \backslash \partial S_i'(t)$ is selected as i's target. If more than one agent simultaneously satisfies this condition, agent i may choose one of them arbitrarily. Hereafter, we describe the time at which i's target is determined as t_i. Once follower i selects its target, it will not be changed. Through this procedure, the spanning tree of $\mathcal{G}(t)$ is constructed.

C. Control Input

Translational velocity input for follower i is designed by the form

$$\boldsymbol{u}_i(t) = u_{ir}(t)\boldsymbol{e}_{ir}(t) + u_{i\theta}(t)\boldsymbol{e}_{i\theta}(t), \quad (17)$$

where agent j is the target of follower i, $\boldsymbol{e}_{ir} = (\boldsymbol{x}_j(t) - \boldsymbol{x}_i(t))/r_{ij}$, and $\boldsymbol{e}_{i\theta}$ is a unit normal vector of $\boldsymbol{e}_{ir}$ (see Fig. 4). The components of translational velocity input u_{ir} and $u_{i\theta}$ are designed as follows:

I) If $\rho_i''' \le r_{ij}(t) \le \rho_i''$:

$$\begin{cases} u_{ir}(t) = a_i'(r_{ij}(t) - \rho_i''), \\ u_{i\theta}(t) = 0. \end{cases} \quad (18)$$

II) If $\rho_i'' < r_{ij}(t) < \rho_i'$ or $t < t_i$:

$$\begin{cases} u_{ir}(t) = 0, \\ u_{i\theta}(t) = 0. \end{cases} \quad (19)$$

III) If $\rho_i' \le r_{ij}(t) < \rho_i' + \frac{U_i'(t)}{2a_i}$:

$$\begin{cases} u_{ir}(t) = a_i(r_{ij}(t) - \rho_i'), \\ u_{i\theta}(t) = \sigma_i u_{ir}(t). \end{cases} \tag{20}$$

IV) If $\rho_i' + \frac{U_i'(t)}{2a_i} \le r_{ij}(t) \le \rho_i' + \frac{U_i'(t)}{a_i}$:

$$\begin{cases} u_{ir}(t) = a_i(r_{ij}(t) - \rho_i'), \\ u_{i\theta}(t) = \sigma_i(U_i'(t) - u_{ir}(t)). \end{cases} \tag{21}$$

Here, $a_i = U_i/(\rho_i - \rho_i')$, $a_i' = V_i/(\rho_i'' - \rho_i''')$, and

$$U_i'(t) = \max_{0 \le \tau \le t} u_{ir}(\tau). \tag{22}$$

With input (18), the follower gets away from the targets when they are too close. Input (19) is introduced for Assumption 1. With (20) and (21), the follower maintains connectivity with its target, while maintaining translational constraints (3) and (4). In case I, we use V_i in a_i', not U_i, in order to make a_i' smaller. This enables us to make the region between ρ_i'' and ρ_i''' smaller. Since our main purpose is to follow the target, this region where the follower tries to keep away from its target should be small.

Note that $r_{ij} \le \rho_i' + U_i'/a_i$ always holds from (20)–(22) as long as agent i is semiconnected with agent j. Moreover, $r_{ij} \ge \rho_i'''$ always holds, as proven in Section IV. Meanwhile, ρ_i', ρ_i'', and ρ_i''' can be chosen arbitrarily as long as conditions (16) hold. Also, $\sigma_i \in [-1, 1]$ is a constant parameter that affects the shape of the swarm. The larger $|\sigma_i|$ is, the wider the shape of the swarm becomes.

Next, rotational speed input $\omega_i(t)$ is designed as follows:

1) If $0 \le t < t_i$:

$$\omega_i(t) = 0. \tag{23}$$

2) If $t_i \le t < t_i'$:

$$\omega_i(t) = \mathrm{sign}(\phi_{ij}(t))B_i(t - t_i). \tag{24}$$

3) If $t \ge t_i'$:

$$\omega_i(t) = k_i\phi_{ij}(t), \tag{25}$$

where t_i' is the time at which input (24) coincides with input (25) for the first time. The feedback gain k_i of input (25) satisfies

$$\frac{K_i}{\psi_i} \le k_i \le \min\left\{\frac{\Omega_i}{\psi_i}, \frac{-K_i + \sqrt{K_i^2 + 4\psi_i B_i}}{2\psi_i}\right\}, \tag{26}$$

where $K_i = \max\{V_i/\rho_i''', (3a_iV_i)/(2a_i\rho_i' + V_i)\}$. Here, input (24) is introduced to obtain wider S_i', which eases the initial state constraint.

Follower i is influenced only by its target j, and with these control laws, follower i can always preserve connectivity with its target and maintain its own physical restrictions. Once the spanning tree of $\mathcal{G}$ is constructed through the target-determination procedure described in Section III-B, each follower preserves semi-connection with its target, which results in connectivity maintenance of the whole swarm.

IV. Analysis of Connectivity and Physical Restriction

In this section, we prove that the swarm keeps LSC, and that all followers satisfy the limitations with the proposed method. Since we mainly consider two agents, i and its target j, for brevity, we hereafter omit the subscripts i and ij for parameters and variables. Let $r_c := \rho' + \frac{U'}{2a}$ and $r_e := \rho' + \frac{U'}{a}$; the velocity of agent j is denoted by

$$\boldsymbol{u}_j = u_{jr}\boldsymbol{e}_r + u_{j\theta}\boldsymbol{e}_\theta. \tag{27}$$

First, we show that the swarm keeps LSC by the control law.

Theorem 1: Under Assumption 1 and control law (18)–(21) and (23)–(25),

$$\rho'' - \frac{U_{n+1}}{a'} < r(t) < \rho' + \frac{U_{n+1}}{a}, \tag{28}$$

$$|\phi(t)| \le \psi, \tag{29}$$

and

$$\|\boldsymbol{u}_i(t)\| < U_{n+1} \tag{30}$$

hold if $\|\boldsymbol{u}_j(t)\| \le U_{n+1}$. Therefore, the swarm keeps LSC.

Proof: First, we show that (28) holds. At $t = t_i$ when the target is determined, $\rho'' \le r \le \rho'$ holds from the target-determining method given in Section III-B. Here, $\dot{r}$ is the relative velocity in the direction of $\boldsymbol{e}_r$ between j and i, denoted by

$$\dot{r} = u_{jr} - u_{ir}. \tag{31}$$

Consider the case of $\rho' \le r \le r_e$. From (20) and (21), (31) yields $\dot{r} = u_{jr} - a(r - \rho')$. This can be easily solved with an initial condition $r(t_i) \le \rho'$ as

$$r(t) \le \rho' + \mathrm{e}^{-at}\int_{t_i}^{t} u_{jr}(\tau)\mathrm{e}^{a\tau}\,\mathrm{d}\tau. \tag{32}$$

Since $u_{jr} \le \|\boldsymbol{u}_j\| \le U_{n+1}$,

$$\begin{aligned} r &\le \rho' + \frac{U_{n+1}}{a}\left(1 - \mathrm{e}^{-a(t-t_i)}\right), \\ &< \rho' + \frac{U_{n+1}}{a}. \end{aligned} \tag{33}$$

In the case of $\rho''' \le r \le \rho''$, noting the initial condition $r(t_i) \ge \rho''$ and $\dot{r} = u_{jr} - a'(r - \rho'')$ from (18), we can easily show that $r > \rho'' - U_{n+1}/a'$ holds in the same way as above. If r becomes (ρ'', ρ') at $t > t_i$ again, we can discuss it in the same way by regarding the time when $r = \rho'$ or $r = \rho''$ as t_i. Therefore, (28) always holds if $\|\boldsymbol{u}_j(t)\| \le U_{n+1}$. Moreover, $r > \rho'' - U_{n+1}/a' \ge \rho'''$ holds from the definition of a', and $V \ge U_{n+1}$, which shows that we don't need control input for $r < \rho'''$.

Next, we show that (30) holds. From (18)–(21) and (28), we have

$$|u_{ir}| < U_{n+1}. \tag{34}$$

Here, we divide the following proof into four cases, which correspond to the cases of translational velocity input in Section III-C.

Case I: From (18), $\|\boldsymbol{u}_i\| = |u_{ir}| < U_{n+1}$.

Case II: From (19), obviously $\|\boldsymbol{u}_i\| = 0 < U_{n+1}$.

Case III: $|u_{ir}| < U'/2$ from (20), and $U' < U_{n+1}$ from (22) and (34). Hence, we have

$$|u_{ir}| < \frac{U_{n+1}}{2}. \tag{35}$$

Considering (35) and $\sigma^2 \le 1$,

$$\|\boldsymbol{u}_i\| = u_{ir}^2 + u_{i\theta}^2 = (1 + \sigma^2)u_{ir}^2 \le 2u_{ir}^2 \le \frac{U_{n+1}^2}{2}. \tag{36}$$

Therefore, we obtain $\|\boldsymbol{u}_i\| \leq U_{n+1}/\sqrt{2} < U_{n+1}$.

Case IV: From (21) and $\sigma^2 \leq 1$,

$$\begin{aligned}\|\boldsymbol{u}_i\|^2 &\leq u_{ir}^2 + (U' - u_{ir})^2 \\ &= 2\left(u_{ir} - \frac{U'}{2}\right)^2 + \frac{U'^2}{2}. \end{aligned} \tag{37}$$

Since $U'/2 \leq |u_{ir}| \leq U'$ from (21) and $U' < U_{n+1}$ from (22), inequality (37) yields $\|\boldsymbol{u}_i\| < U_{n+1}$.

Now we show that (29) holds, using (30). Due to the symmetry of (23)–(25) with regard to $\phi = 0$, we hereafter consider the case of $\phi \geq 0$ and $t \geq t_i$ at which the target is already determined. The time derivative of ϕ is $\dot{\phi} = \omega' - \omega$, where

$$\omega' := \frac{1}{r}(u_{j\theta} - u_{i\theta}). \tag{38}$$

1) *If* $t_i \leq t < t_i'$: $\phi(t_i) \leq \psi' < \psi$ holds from the target-determination method. From (24), we have $\dot{\phi} = \omega' - B(t - t_i)$. Here,

$$\omega' \leq \frac{U_{n+1}}{\rho'''} \tag{39}$$

holds from (18), (19), and $\|\boldsymbol{u}_j\| \leq U_{n+1}$ in Case I and II;

$$\omega' \leq \max\left\{\frac{U_{n+1}}{\rho'}, \frac{3aU_{n+1}}{2a\rho' + U_{n+1}}\right\} \tag{40}$$

holds from (20), (21), and $\|\boldsymbol{u}_j\| \leq U_{n+1}$ in Case III and IV. Hence, we have

$$\omega' \leq \max\left\{\frac{U_{n+1}}{\rho'''}, \frac{3aU_{n+1}}{2a\rho' + U_{n+1}}\right\} \leq K. \tag{41}$$

The second inequality of (41) is derived from $V \geq U_{n+1}$. Thus, we have $\dot{\phi} \leq K - B(t - t_i)$. When the right side of this inequality is zero, $t = t_i + K/B$. Therefore, from $\phi(t_i) \leq \psi'$ and (10),

$$\begin{aligned}\phi \leq\ & \phi(t_i) + \int_{t_i}^{t_i + \frac{K}{B}} \{K - B(\tau - t_i)\}\,\mathrm{d}\tau \\ \leq\ & \psi' + \frac{K^2}{2B} = \psi. \end{aligned} \tag{42}$$

2) *If* $t \geq t_i'$: From (25) and $\|\boldsymbol{u}_j\| \leq U_{n+1}$, we have $\dot{\phi} = \omega' - k\phi \leq K - k\phi$. Considering the range of k (26), when $\phi = \psi$, this yields

$$\dot{\phi} \leq K - k\psi \leq 0. \tag{43}$$

Thus, $\phi > \psi$ will never hold.

In the case of $\phi \leq 0$, we can prove that $\phi \geq -\psi$ holds the same way. Hence, (29) always holds if $\|\boldsymbol{u}_j\| \leq U_{n+1}$.

Finally, we show that the swarm keeps LSC. From Assumption 1, the leader is the first in the swarm to move, while the other agents are stationary. Next, at least one follower sets the leader as its target, as described in Section III-B. Let agent i be an agent whose target is the leader $n+1$. Since we have (11), (28) gives $r < \rho' + U_i/a = \rho$. This and (29) shows that the ji semi-connection is always maintained, where $j = n+1$. As agent i moves to follow j, an agent l sets i or $n+1$ as its target l'. Since $\|\boldsymbol{u}_i\| < U_{n+1}$ from (30), we can apply the same argument for j and i to l' and l. Moreover, we can consider any pair of such agents m' and m the same way. Here, note that Assumption 1 and the target determination described in subSection III-B ensures every follower can determine its target, and the target is LSC. Therefore, the swarm composes the spanning tree and maintains it, which means the swarm keeps LSC. ■

Next, we show that all followers satisfy the physical limitations (3)–(7).

Theorem 2: Under Assumption 1 and control law (18)–(21) and (23)–(25), the physical limitations (3)–(7) are satisfied.

Proof: We have proven that the limitation (3) is satisfied in Theorem 1. In addition, from (29) and control input (23)–(25), it is obvious that the rotational speed restriction (5) is satisfied for every follower. In the following, we consider (4), (6), and (7). For the following proofs, we assume that $\|\boldsymbol{u}_j(t)\| \leq U_{n+1}$ holds.

First we consider (7). It is necessary to show that $\boldsymbol{u}_i(t)$ and $\omega(t)$ are continuous at any $t \geq 0$. As to $\boldsymbol{u}_i$, for $t < t_i$, $\boldsymbol{u}_i \equiv \boldsymbol{0}$ is continuous. For $t \geq t_i$, since $u_{jr} \leq U_{n+1}$ and $u_{ir} < U_{n+1}$ from (30), $\dot{r}$ is always finite. Hence, r is continuous at any $t \geq t_i$. Moreover, since u_{ir} and $u_{i\theta}$ are continuous for r from definitions (18)–(21), they are continuous for t. Now we consider the basis vectors $\boldsymbol{e}_r$ and $\boldsymbol{e}_\theta$. The angular velocity of $\boldsymbol{e}_r$ and $\boldsymbol{e}_\theta$ is denoted by ω', and their time-derivatives are

$$\dot{\boldsymbol{e}}_r = \omega' \boldsymbol{e}_\theta,\ \dot{\boldsymbol{e}}_\theta = -\omega' \boldsymbol{e}_r, \tag{44}$$

by which we find that $\boldsymbol{e}_r$ and $\boldsymbol{e}_\theta$ are continuous. Thus, we have found that $\boldsymbol{u}_i$ is always continuous.

Next, we consider ω. From $|\omega| \leq \Omega$ and $r > \rho'''$, $\dot{\phi} = \omega' - \omega$ is finite. This shows that ϕ is continuous, and thus, (25) is continuous. Both (23) and (24) are obviously continuous. Moreover, (23) and (24) are continuous at $t = t_i$, and (24) and (25) are continuous at $t = t_i'$. Hence, it is proven that $\omega(t)$ is always continuous.

Next, we show that physical restriction (4) holds. Since $\|\dot{\boldsymbol{u}}_i\| \equiv \boldsymbol{0}$ at $t < t_i$, we hereafter consider $t \geq t_i$. Substituting (44) into the time-derivative of (17), acceleration of follower i is computed as

$$\dot{\boldsymbol{u}}_i = (\dot{u}_{ir} - u_{i\theta}\omega')\,\boldsymbol{e}_r + (\dot{u}_{i\theta} + u_{ir}\omega')\,\boldsymbol{e}_\theta. \tag{45}$$

The norm of the acceleration of follower i is calculated as

$$\|\dot{\boldsymbol{u}}_i\|^2 = (\dot{u}_{ir}^2 + \dot{u}_{i\theta}^2) + \omega'^2(u_{ir}^2 + u_{i\theta}^2) + 2\omega'(u_{ir}\dot{u}_{i\theta} - u_{i\theta}\dot{u}_{ir}) \tag{46}$$

from (45),

Case I: From (15), (16), (18), (28), (30), (31), and(38),

$$\begin{aligned}||\dot{\boldsymbol{u}}_i||^2 =\ & \dot{u}_{ir}^2 + u_{ir}^2 \frac{u_{j\theta}^2}{r^2} \\ =\ & a'^2(u_{jr} - u_{ir})^2 + a'^2(r - \rho'')^2 \frac{u_{j\theta}^2}{r^2} \\ <\ & a'^2\{(|u_{jr}| + U_{n+1})^2 + \frac{(\rho''' - \rho'')^2}{\rho'''^2} u_{j\theta}^2\} \\ \leq\ & a'^2\{(|u_{jr}| + U_{n+1})^2 + 2u_{j\theta}^2\} \\ \leq\ & a'^2\{(|u_{jr}| + U_{n+1})^2 + 2(U_{n+1}^2 - u_{jr}^2)\} \\ \leq\ & 4a'^2 U_{n+1}^2 \\ \leq\ & A^2. \end{aligned} \tag{47}$$

Case II: Obviously $\|\dot{\boldsymbol{u}}_i\| = 0 < A_i$ from (19).

Case III: From (20), (31), (38), and $\sigma^2 \leq 1$, we have

$$\begin{aligned}\|\dot{\boldsymbol{u}}_i\|^2 &= \left(1+\sigma^2\right) a^2 \Bigg\{ \left(u_{jr}-u_{ir}\right)^2 \\ &\quad + \left(u_{j\theta}-u_{i\theta}\right)^2 \frac{\left(r-\rho'\right)^2}{r^2} \Bigg\} + 2\omega \cdot 0 \\ &< 2a^2 \left\{ \left(u_{jr}-u_{ir}\right)^2 + \left(u_{j\theta}-u_{i\theta}\right)^2 \right\} \\ &\quad - 2u_{ir}\left(u_{jr}+\sigma u_{j\theta}\right) \Big\} \\ &\leq 2a^2 \left\{ \left(u_{jr}^2+u_{j\theta}^2\right) + 2u_{ir}^2 + 2u_{ir}\left(|u_{jr}|+|u_{j\theta}|\right) \right\}.\end{aligned}$$

This inequality yields $\|\dot{\boldsymbol{u}}_i\|^2 < (1+\sqrt{2})^2 a^2 U_{n+1}^2$ since $u_{jr}^2 + u_{j\theta}^2 \leq U_{n+1}^2$, $|u_{jr}| + |u_{j\theta}| \leq \sqrt{2} U_{n+1}$ using the Lagrange multiplier, and (35). Thus, from (12), we obtain

$$\|\dot{\boldsymbol{u}}_i\| < \left(1+\sqrt{2}\right) a U_{n+1} < A_i. \tag{48}$$

Case IV: From (21), (31), and (38), we have

$$\begin{aligned}\|\dot{\boldsymbol{u}}_i\|^2 &= (1+\sigma^2) a^2 (u_{jr}-u_{ir})^2 \\ &\quad - \frac{2a}{r}(u_{jr}-u_{ir})(u_{j\theta}-u_{i\theta})(\sigma u_{ir}+u_{i\theta}) \\ &\quad + \frac{1}{r^2}(u_{j\theta}-u_{i\theta})^2 (u_{ir}^2+u_{i\theta}^2).\end{aligned}$$

Since $r = \rho' + u_{ir}/a > u_{ir}/a$ from (21), $u_{ir} \geq u_{i\theta}$, and $\sigma^2 \leq 1$,

$$\begin{aligned}\|\dot{\boldsymbol{u}}_i\|^2 &< a^2 \Bigg\{ 2(u_{jr}-u_{ir})^2 \\ &\quad + 2|u_{jr}-u_{ir}||u_{j\theta}-u_{i\theta}| \frac{u_{ir}+u_{i\theta}}{u_{ir}} \\ &\quad + (u_{j\theta}-u_{i\theta})^2 \frac{(u_{ir}^2+u_{i\theta}^2)}{u_{ir}^2} \Bigg\} \\ &\leq 2a^2 (|u_{jr}-u_{ir}| + |u_{j\theta}-u_{i\theta}|)^2 \\ &\leq 2a^2 (|u_{ir}| + |u_{i\theta}| + |u_{jr}| + |u_{j\theta}|)^2.\end{aligned}$$

Substituting $|u_{ir}| + |u_{i\theta}| \leq U' < U_{n+1}$ from (21), and $|u_{jr}| + |u_{j\theta}| \leq \sqrt{2} U_{n+1}$ as the third case, we obtain $\|\dot{\boldsymbol{u}}_i\|^2 < (2+\sqrt{2})^2 a^2 U_{n+1}^2$. Thus, from (12),

$$\|\dot{\boldsymbol{u}}_i\| < (2+\sqrt{2}) a U_{n+1} \leq A_i. \tag{49}$$

From above, (4) always holds.

Finally, we show that the last limitation (6) holds. Obviously, $|\dot{\omega}| = 0$ if $t < t_i$, and $|\dot{\omega}| = B$ if $t_i \leq t < t_i'$. So, we hereafter consider the case of $t \geq t_i'$. From (25), (29), and (41), we have

$$|\dot{\omega}| = k\,|\omega' - k\phi| \leq k(K + k\psi). \tag{50}$$

In order for this to be less than or equal to B, it requires

$$0 < k \leq \frac{-K + \sqrt{K^2 + 4\psi B}}{2\psi}. \tag{51}$$

This is satisfied from the condition for k (26). In addition, k that satisfies (26) exists as long as constraints (13) and (14) hold. Thus, $|\dot{\omega}| \leq B$ always holds.

TABLE I
SPECIFICATIONS OF FOLLOWERS IN THE SIMULATION

i	1	2	3	4	5	6	7	8	9
ρ_i [m]	4.1	6.7	4.7	7.0	4.8	5.3	6.2	5.9	5.0
ρ_i' [m]	1.3	1.3	1.3	1.3	1.3	1.3	1.3	1.3	1.3
ρ_i'' [m]	1.0	1.0	1.0	1.0	1.0	1.0	1.0	1.0	1.0
ψ_i [rad]	$\pi/6$	$\pi/6$	$\pi/5$	$\pi/7$	$\pi/6$	$\pi/5$	$\pi/6$	$\pi/5$	$\pi/7$
U_i [m/s]	0.52	0.90	0.70	0.76	0.60	0.71	0.85	0.60	0.59
A_i [m/s^2]	0.30	0.40	0.50	0.60	0.50	0.50	0.90	0.90	0.70
Ω_i [rad/s]	$3\pi/4$	$2\pi/3$	$2\pi/3$	$\pi/2$	$2\pi/3$	$2\pi/3$	$\pi/2$	$2\pi/3$	$3\pi/4$
B_i [rad/s^2]	π	$3\pi/4$	$3\pi/4$	$\pi/2$	$2\pi/3$	$3\pi/4$	π	$\pi/2$	π
σ_i	0.2	−0.2	0	1.0	0.8	0.6	−1.0	−0.8	−0.6
V_i [m/s]	0.30	0.34	0.38	0.35	0.36	0.38	0.47	0.42	0.42
ρ_i''' [m]	0.41	0.43	0.43	0.59	0.48	0.44	0.52	0.60	0.50
k_i	1.37	1.50	1.37	1.32	1.41	1.37	1.73	1.12	1.87

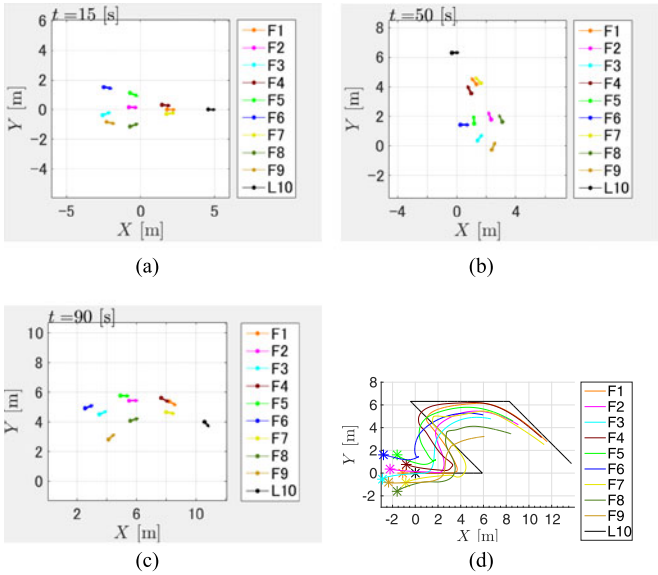

Fig. 5. (a)–(c) Screenshots, and (d) paths of all agents in the simulation. (a) $t = 15$ s. (b) $t = 50$ s. (c) $t = 90$ s. (d) Paths of all agents. The asterisks show the initial positions.

Finally, Theorem 1 (see (30)) shows that all agents move under the speed of the leader. From this fact, the condition $\|\boldsymbol{u}_j\| \leq U_{n+1}$ holds for any follower. Thus, we find that (3)–(7) are satisfied if the leader moves under restrictions (11)–(14). ■

V. SIMULATION

In this section, we present the results of a simulation with ten agents. The specifications of the followers are listed in Table I. From (11)–(15), the speed restriction of the leader was computed to be 0.296 m/s. The leader moves for 105 s, and makes some sharp turns at $t = 20, 50$, and 79 s, which require the followers to make large accelerations. Fig. 5 contains screenshots and shows the trajectory of the experiment. In Fig. 5(a)–(c), the arrow shows the orientation of the agents. We do not consider the orientation of the leader, so the leader's arrow shows its moving direction. In the legend, L10 is the leader, and F1, F2, . . ., F9 are the followers.

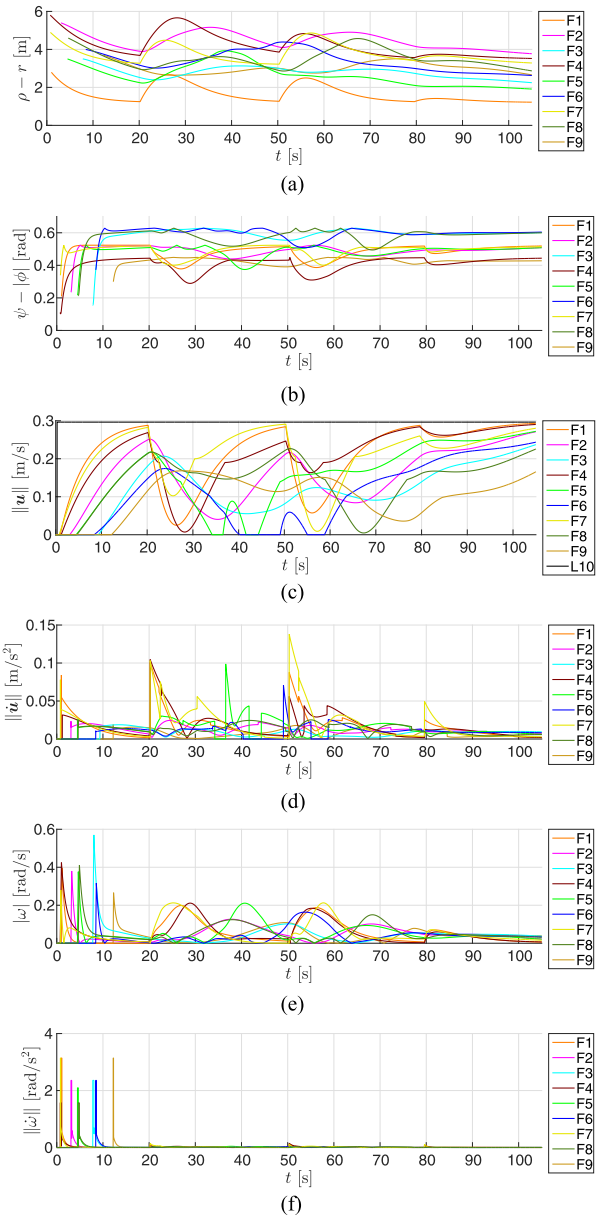

Fig. 6. Results of the simulation. (a) Connection margin $\rho - r$ of all followers. (b) [Connection margin $\psi - |\phi|$ of all followers. (c) Norm of translational velocity input of all agents. (d) Norm of translational acceleration of all followers. (e) Norm of angular velocity input of all followers. (f) Norm of angular acceleration of all followers.

TABLE II
SPECIFICATIONS OF FOLLOWERS IN THE EXPERIMENT

i	1	2	3
ρ_i [m]	1.2	1.0	1.1
ρ_i' [m]	0.6	0.6	0.55
ρ_i'' [m]	0.40	0.40	0.35
ψ_i [rad]	$\pi/6$	$\pi/6$	$\pi/5$
U_i [m/s]	0.20	0.20	0.25
A_i [m/s^2]	0.60	0.50	0.80
Ω_i [rad/s]	$\pi/3$	$\pi/3$	$2\pi/5$
B_i [rad/s^2]	$2\pi/3$	$\pi/2$	$\pi/2$
σ_i	-0.8	0.7	-0.5
V_i [m/s]	0.19	0.18	0.19
ρ_i''' [m]	0.28	0.28	0.26
k_i	1.34	1.22	1.12

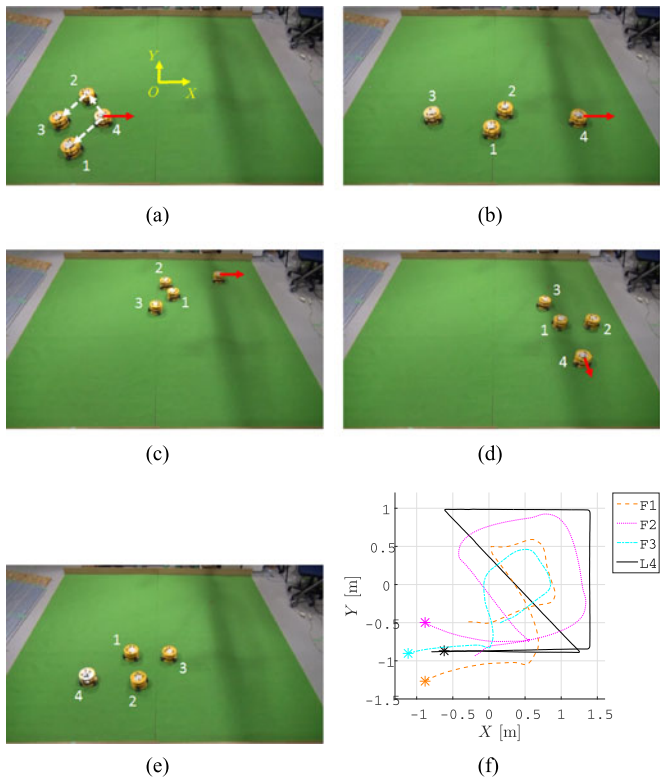

Fig. 7. (a)–(e) Screenshots, and (f) paths of all agents in the experiment. (a) The initial configuration. (b) $t = 10$ s. (c) $t = 45$ s. (d) $t = 60$ s. (e) $t = 82$ s. The leader has stopped. (f) Paths of all agents. The asterisks show the initial positions.

The results are shown in Fig. 6. Fig. 6(a) and (b) show the connection margins $\rho - r$ and $\psi - |\phi|$, respectively. Since both connection margins were always positive for all followers, we found that the swarm maintained LSC. Moreover, checking Fig. 5(c)–(f) against Table I, we found that all followers satisfied all physical limitations.

VI. EXPERIMENT

In this section, we show the results of an experiment with real robots to confirm the effectiveness of our method.

The robots were omni-directional, and controlled by velocity commands via Bluetooth. In order to measure the positions of the robots, we used a motion-capture system that included high-speed cameras and tracking software. Although the system itself was centrally controlled, the controller for each agent used only locally available information. In this respect, the controller in this experiment was decentralized.

In the experiment, we observed the motion of three followers when the leader performed some sharp turns at $t = 12$, 35, 47, and 58 s. The motion of the leader required the followers to make large accelerations. The sampling time was 0.1 s, and the leader moved for 71 s. The specifications of the followers are listed in Table II From (11)–(15), the speed restriction of the leader was computed to be 0.177 m/s. Fig. 7 contains screenshots and

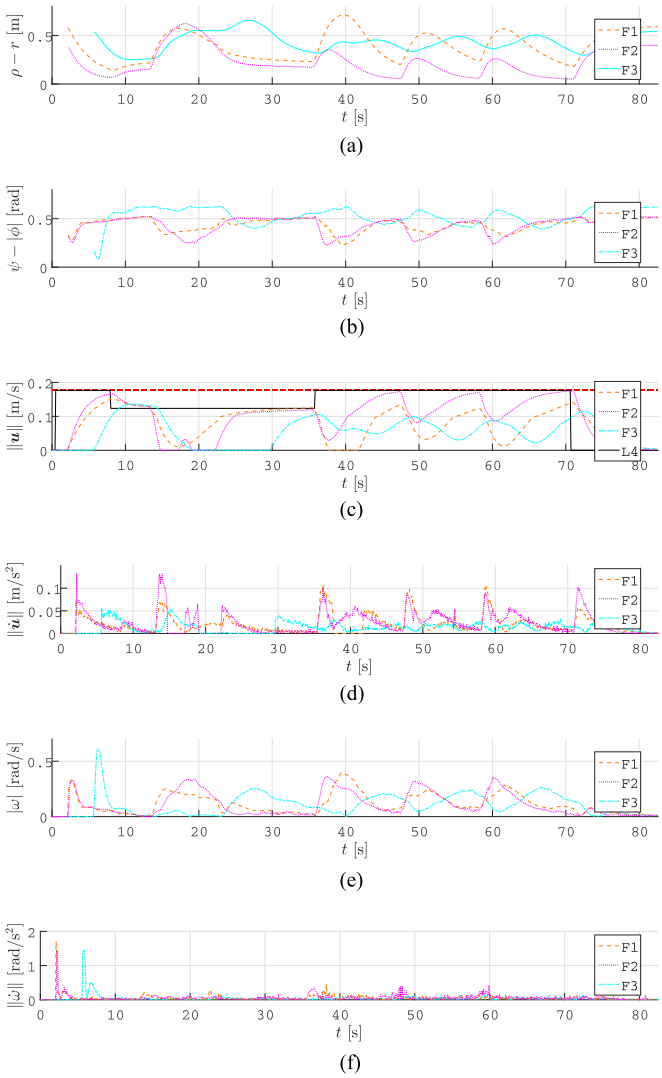

Fig. 8. Results of the experiment. (a) Connection margin $\rho - r$ of all followers. (b) Connection margin $\psi - |\phi|$ of all followers. (c) Norm of translational velocity input of all agents. (d) Norm of translational acceleration of all followers. (e) Norm of angular velocity input of all followers. (f) Norm of angular acceleration of all followers.

shows the trajectory of the experiment. The red arrows in the screenshots show the leader's moving directions, and in Fig. 7(f), L4 is the leader, and F1, F2, and F3 are the followers.

The results are shown in Fig. 8. Fig. 8(a) and (b) show the connection margins $\rho - r$ and $\psi - |\phi|$, respectively. Since both connection margins were always positive for all followers, we found that the swarm maintained LSC. Moreover, checking Fig. 8(c)–(f) against Table I, we found that all followers satisfied all physical limitations. Note that the translational and angular velocities are respective inputs, and the translational and angular accelerations are numerical time-derivatives of the inputs, respectively.

VII. Conclusion

This letter proposed a method in which a leader was able to navigate a heterogeneous robotic swarm. In our strategy, each follower, which has its own unique specifications, distributedly determines a robot to follow and keeps semi-connected with it to construct the spanning tree of the swarm. Since each agent is controlled by information that is locally available, our method is decentralized. We proved that connectivity maintenance was achieved while each follower kept within its own unique physical limitations. To validate our method, we performed a simulation and an experiment with real robots and confirmed its feasibility.

In future work, we will investigate collision avoidance and maintaining Line of Sight between robots by designing the $\boldsymbol{e}_\theta$ component of translational velocity input, which means designing σ_i as a variable. We will also seek proof of convergence of the swarm shape.

References

[1] M. Brambilla, E. Ferrante, M. Birattari, and M. Dorigo, "Swarm robotics: A review from the swarm engineering perspective," *Swarm Intell.*, vol. 7, no. 1, pp. 1–41, 2013.

[2] L. Bayindir, "A review of swarm robotics tasks," *Neurocomputing*, vol. 172, pp. 292–321, 2016.

[3] I. Navarro and F. Matia, "A survey of collective movement of mobile robots," *Int. J. Adv. Robot. Syst.*, vol. 10, pp. 1–9, 2013.

[4] Y. Dai, Y. Kim, S. Wee, D. Lee, and S. Lee, "A switching formation strategy for obstacle avoidance of a multi-robot system based on robot priority model," *ISA Trans.*, vol. 56, pp. 123–134, 2015.

[5] Y. Kantaros, M. Thanou, and A. Tzes, "Distributed coverage control for concave areas by a heterogeneous robot-swarm with visibility sensing constraints," *Automatica*, vol. 53, pp. 195–207, 2015.

[6] D. Saldana, R. J. Alitappeh, L. C. A. Pimenta, and R. Assuncao, "Dynamic perimeter surveillance with a team of robots," in *Proc. IEEE Int. Conf. Robot. Autom.*, 2016, pp. 5289–5294.

[7] T. Kim and T. Sugie, "Cooperative control for target-capturing task based on a cyclic pursuit strategy," *Automatica*, vol. 43, pp. 1426–1431, 2007.

[8] J. Chen, M. Gauci, and R. Grob, "A strategy for transporting tall objects with a swarm of miniature mobile robots," in *Proc. IEEE Int. Conf. Robot. Autom.*, 2013, pp. 863–869.

[9] R. Olfati-Saber, "Flocking for multi-agent dynamic systems: Algorithms and theory," *IEEE Trans. Autom. Control*, vol. 51, no. 3, pp. 401–420, Mar. 2006.

[10] A. Cezayirli and F. Keresteciogl, "Navigation of non-communicating autonomous mobile robots with guaranteed connectivity," *Robotica*, vol. 31, no. 5, pp. 767–776, 2013.

[11] F. Bullo, J. Cortes, and S. Martinez, *Distributed Control of Robotic Networks: A Mathematical Approach to Motion Coordination Algorithms*. Princeton, NJ, USA: Princeton Univ. Press, 2009.

[12] M. Dorigo *et al.*, "Swarmanoid: A novel concept for the study of heterogeneous robotic swarm," *IEEE Robot Autom. Mag.*, vol. 20, no. 4, pp. 60–71, Dec. 2013.

[13] C. McCook and J. Esposito, "Flocking for heterogeneous robot swarms: A military convoy scenario," in *Proc. 39th Southeastern Symp. Syst. Theory*, 2007, pp. 26–31.

[14] L. Sabattini, C. Secchi, and N. Chopra, "Decentralized estimation and control for preserving the connectivity of directed graphs," *IEEE Trans. Cybern.*, vol. 45, no. 10, pp. 2273–2286, Oct. 2015.

[15] D. Panagou and V. Kumar, "Cooperative visibility maintenance for leader-follower formations in obstacle environments," *IEEE Trans. Robot.*, vol. 30, no. 4, pp. 831–844, Aug. 2014.

[16] C. K. Verginis, C. P. Bechlioulis, D. V. Dimarogonas, and K. J. Kyriakopoulos, "Decentralized 2-D control of vehicular platoons under limited visual feedback," in *Proc. IEEE/RSJ Int. Conf. Intell. Robot. Syst.*, 2015, pp. 3566–3571.

[17] C. F. Ardito, D. D. Paola, and A. Gasparri, "Decentralized estimation of the minimum strongly connected subdigraph for robotic networks with limited field of view," in *Proc. 51st IEEE Conf. Decis. Control*, 2012, pp. 5304–5309.